# Short-term dynamics of a mixed chemical and electrical synapse in a rhythmic network

**A. Mamiya[1], Y. Manor[2] and F. Nadim[3]**

[1] Center for Molecular and Behavioral Neuroscience
Rutgers University, Newark, NJ 07102

[2] Life Sciences Department and
Zlotowski Center for Neurosciences
Ben-Gurion University of the Negev
Beer-Sheva, Israel 84105

[3] Department of Mathematical Sciences
Center for Applied Mathematics and Statistics
New Jersey Institute of Technology and
Department of Biological Sciences
Rutgers University, Newark, NJ 07102

CAMS Report 0203-15, Spring 2003

Center for Applied Mathematics and Statistics

NJIT

Section: Behavioral/Systems Neuroscience

Section Editor: Dr. Stephen G. Lisberger

# Short-term dynamics of a mixed chemical and electrical synapse in a rhythmic network

Akira Mamiya
Center for Molecular and Behavioral Neuroscience, Rutgers University, Newark, NJ 07102. mamiya@axon.rutgers.edu

Yair Manor
Life Sciences Department and Zlotowski Center for Neurosciences, Ben-Gurion University of the Negev, Beer-Sheva, Israel 84105. yairman@bgumail.bgu.ac.il

Farzan Nadim
Department of Mathematical Sciences, New Jersey Institute of Technology and Department of Biological Sciences, Rutgers University, Newark, NJ 07102. farzan@njit.edu

Abbreviated title: Dynamics of a mixed synapse in a rhythmic network

Number of pages in Text:
Number of words in Abstract:
Number of words in Introduction:
Number of words in Discussion:
Number of Figures: 7
Number of Tables: 0

**Corresponding Author**:

Farzan Nadim, Department of Biological Sciences, 101 Warren St., Newark, NJ 07102, Phone (973) 353-1541, Fax (973) 353-1007, Email: farzan@njit.edu

**Acknowledgments:**

This research was supported by US-Israel Binational Science Foundation (2001-039 YM&FN) and NIMH60605-01 (FN)

**Key Words:** Synaptic depression, synaptic dynamics, stomatogastric ganglion, oscillations, central pattern generator, motor system

## Abstract

In the rhythmically active pyloric circuit of the spiny lobster, the synapse between the lateral pyloric (LP) neuron and pyloric constrictor (PY) neurons has an inhibitory depressing chemical and an electrical component. We characterized the dynamics of the LP to PY synapse after blocking the rhythmic activity and correlate these dynamics with the relative timing of activity of these two neurons before the rhythm was blocked. When a train of voltage pulses was applied to the voltage-clamped LP neuron, the inhibitory chemical component of the postsynaptic potential (PSP) in the PY neuron rapidly depressed. Thus, after the first few pulses, the PSP was either hyperpolarizing or depolarizing depending on the interpulse duration, with higher interpulse durations producing depolarizing PSPs. To characterize the synaptic response during rhythmic activity, we played back pre-recorded realistic waveforms in the voltage-clamped LP neuron. After an initial transient, the resulting PSP in PY was always depolarizing, suggesting that in an ongoing rhythm the electrical component of the synapse is dominant. However, using pharmacological tools we unmasked a significant contribution of the chemical component of the synapse to the fine-tuning of the PY PSP. Our results indicate that the chemical component of the mixed synapse acts to delay the peak time of the PSP and to reduce its amplitude, and that these effects become more important at slower cycle periods. We then compared the properties of the synapse as measured in the quiescent preparation with the relative activity phase of the LP and PY neurons in the ongoing pyloric rhythm. Interestingly, the phase between the LP waveform and the PY PSP correlated well with the phase between the LP and PY bursts in the ongoing rhythm. This suggests that mixed synapses may dynamically affect the phase between two neurons if the rhythm frequency is altered.

## Introduction

Neurons coupled with electrical synapses often form chemical synapses as well (Michelson and Wong, 1994; Benardo, 1997; Gibson et al., 1999; Mann-Metzer and Yarom, 1999; Fukuda and Kosaka, 2000). The composite “mixed synapse” is considered a single functional unit. Several studies have proposed that mixed synapses act to synchronize the firing of neurons (Benardo, 1997; Galarreta and Hestrin, 1999; Tamas et al., 2000), or serve as a coincidence-detection mechanism of excitatory inputs (Galarreta and Hestrin, 2001a). Mixed synapses have also been implicated in neuronal rhythmogenesis (Galarreta and Hestrin, 2001b). In many mixed synapses, the chemical component shows short-term facilitation or depression, whereas the effect of electrical synapses is less use-dependent (Galarreta and Hestrin, 1999; Gibson et al., 1999; Tamas et al., 2000). Thus, a mixed synapse might dynamically change its properties in response to a modification in the frequency or pattern of activation of the synapse (Galarreta and Hestrin, 2001b).

We explore this possibility using the rhythmically active pyloric network (frequency: 0.5-2 Hz) of the spiny lobster *Panulirus interruptus*. The pyloric rhythm is generated by a pacemaker ensemble of an Anterior Burster (AB) and two Pyloric Dilator (PD) neurons. The remaining (follower) neurons are coupled to the pacemaker neurons with electrical and inhibitory chemical synapses. The period and activity phase of pyloric neurons are determined by the intrinsic properties of these neurons as well as the dynamics of the synapses among them (Nusbaum and Beenhakker, 2002).

An important property of the pyloric network is that the relative phase of activity of different neurons in the network is adjusted depending on the cycle frequency to maintain a stable triphasic pattern (Miller and Selverston, 1982). Two classes of follower neurons, the Lateral Pyloric (LP) and Pyloric Constrictor (PY) neurons are reciprocally coupled via mixed synapses. In the transmission of signals from LP to PY, the two components of the mixed synapse have opposite effects. When the LP neuron bursts, the electrical component promotes PY neuron activity whereas the chemical component acts to suppress it. Moreover, previous studies have shown that the relative phase of activity of the LP and PY neurons was well maintained when the frequency of the pyloric rhythm was altered by external manipulation (Hooper, 1997a; 1997b).

In this study, we explore the complex interaction between electrical and inhibitory chemical components in the LP to PY synapse. We first characterize parameters describing the dynamics of the synapse (amplitude and the extent and time constant of depression) by suppressing the pyloric activity, voltage clamping the LP neuron with trains of voltage pulses and recording the postsynaptic potential (PSP) in the PY neuron. After determining the synaptic parameters, we describe the synaptic activity in the context of the rhythmic pyloric rhythm. This is done by playing back pre-recorded realistic waveforms in the voltage-clamped LP neuron and recording the PSP. Finally, using correlation analysis, we show that the frequency-dependent properties of the LP to PY mixed synapse are important in determining the firing phase of the PY neurons during rhythmic activity. These results indicate that dynamical properties of a mixed synapse can serve as a mechanism for fine-tuning of phasing in oscillatory networks.

**Materials and Methods**

All experiments were done on adult spiny lobsters *Panulirus interruptus* (Don Tomlinson, San Diego, CA). The stomatogastric nervous system (STNS) was isolated with standard procedures (Selverston et al., 1976; Harris-Warrick et al., 1992). The isolated STNS was pinned down on a Sylgard-coated petri dish, and superfused with chilled (16°C) physiological saline containing (in mM: 479.0 NaCl; 12.9 KCL; 13.7 $CaCl_2 \bullet 2H_2O$; 10.0 $MgSO_4 \bullet 7H_2O$; 3.9 $NaSO_4 \bullet 10H_2O$; 11.2 Trizma base; 5.1 Maleic acid, pH=7.45).

Pyloric neurons were identified by their stereotypical axonal projections in identified nerves using conventional techniques (Selverston et al., 1976; Harris-Warrick et al., 1992). The pyloric activity was monitored with stainless steel wire electrodes from identified nerves. Extracellular signals were amplified with a differential AC amplifier model 1700 (A-M systems, Carlsborg, WA). Intracellular recordings were made by impaling the soma with sharp microelectrodes filled with 0.6 M $K_2SO_4$ + 20 mM KCL (25-35 MΩ for identification of neurons and recording the postsynaptic neuron) or 3M KCL (8-12 MΩ for current injection in the presynaptic neuron). All intracellular recordings were done with Axoclamp 2B amplifiers (Axon Instruments, Inc, Foster City, CA).

Synaptic potentials were measured after abolishing the pyloric activity. This was done by bath application of 0.1 μM tetrodotoxin (TTX; Biotium, CA) to block both descending inputs to and activity within the stomatogastric ganglion. Synaptic activity was studied by voltage clamping the presynaptic neuron using a series of voltage pulses, or realistic waveforms from a holding potential of –60 mV. The postsynaptic response was monitored in current clamp mode. The LP to PY synapse has both electrical and chemical components. Since there is no known specific blocker for the electrical coupling in this system, the chemical component was estimated by subtracting the postsynaptic potential recorded after blocking the chemical synapse from that recorded in control conditions. The chemical synapse was blocked by bath application of 10 μM picrotoxin (PTX) (Marder and Paupardin-Tritsch, 1978).

Realistic waveforms were constructed by recording voltage traces of the LP neuron in an on-going rhythm. In order to obtain typical LP waveforms at different pyloric periods, we injected current into one of the pacemaker group neurons (AB/PD) to change the period. We chose two representative cases, with short (625 ms) and long (1600 ms) periods. For each case, we low-pass filtered the trace at 10 Hz (to remove action potentials), divided the trace to single cycles and averaged these cycles to construct a unitary waveform. In a quiescent LP neuron, we repeatedly injected the unitary waveform to stimulate the LP neuron with a realistic waveform. Manipulations of traces (waveform cutting, low pass filtering and averaging) were done with a custom-made program written in Labwindows/CVI (National Instruments, Houston, TX).

All intracellular recordings were digitized at 4kHz and stored on a PC using a PCI-MIO-16E-1 board (National Instruments, Houston, TX) and custom-made recording software written in Labwindows/CVI (National Instruments, House, TX). All analysis, such as detection of the peak time and the amplitude of the postsynaptic response, averaging the synaptic response, calculation of the ratios, digital subtraction of the traces, and curve fitting were done by custom-made programs written in Matlab (Math Works Inc., Natick, MA). Statistical tests were done using SAS package (SAS Institute Inc., Cary, NC).

## Results

Neurons that participate in the pyloric rhythm fire bursts of action potentials in three distinct phases. The pacemaker AB and PD neurons fire in-phase, followed, after a short delay, by a burst of action potentials in the LP neuron and then followed, with some overlap, by bursts of action potentials in the PY neurons (Fig. 1A). The period and firing phases of neurons in the pyloric network are determined by the intrinsic properties of these neurons as well as the dynamics of the synapses among them (Nusbaum and Beenhakker, 2002). Figure 1B shows the connectivity among the AB, PD, LP and PY neurons. In this study, we explore the interaction between electrical and inhibitory chemical components of the mixed synapse between the LP and PY neurons. Previous studies have shown that the electrical component of this synapse is rectifying: it allows preferential flow of positive current from LP to PY (Graubard and Hartline, 1987; Johnson et al., 1993). We show that the inhibitory chemical component of this synapse is strongly depressing and examine the dynamics resulting from the combination of these two components.

This study was done in three steps. First, we obtained the parameters to describe dynamics of the LP to PY synapse by using trains of voltage pulses. Next, we compared these parameters with the burst timing of the postsynaptic PY neuron during the ongoing rhythm to look for the functional significance of the synaptic dynamics. Figure 1C shows how the burst onset phase was calculated for each PY neuron. The burst onset phase was defined as the time difference $\Delta T$ between the LP neuron burst onset and the PY neuron burst onset, divided by the ongoing pyloric cycle period ($P_{natural}$). Finally, we examined dynamics and function of the LP to PY synapse in a setting closer to that of an ongoing rhythm by voltage clamping the LP neuron using pre-recorded realistic waveforms, and comparing the timing of the PSP with the burst timing of the postsynaptic PY neuron.

### *Characterization of the dynamics of the LP to PY synapse with trains of voltage pulses*

To study the dynamic properties of the LP to PY synapse and to determine the parameters for these dynamics (for example magnitude of depression and time course of recovery), we first activated the synapse with train of voltage pulses and examined the dynamics of PSP. Measurements of PSPs were performed after abolishing the ongoing activity. To separate the chemical and electrical components of the PSP, we compared the response of the PY neuron in control and in the presence of 10 μM picrotoxin (PTX).

Figure 2A is an example showing voltage traces of the LP and PY neurons under this paradigm. In this example, both the pulse and the interpulse durations were 400 ms. The top trace shows the response of the PY neuron in control (Ctl) conditions. The second trace is the PY response in the presence of picrotoxin (PTX) and represents the electrical component of the synapse. The chemical

component of the synapse was approximated by subtracting the second trace from the first trace (third trace, Ctl-PTX).

In control saline, the PY response to the first pulse consisted of 3 phases: a brief and small depolarization, a 2 mV hyperpolarization that peaked at 60 ms, and a depolarization that was truncated at the end of the pulse. In subsequent pulses, the membrane potential of the PY neuron was purely depolarizing and reached steady state near the end of the pulse. The depolarizing and hyperpolarizing phases of the PY response were due to the electrical and chemical components of the LP and PY synapse, respectively. In PTX, all five pulses in the LP neuron produced depolarizing responses in the PY neuron, each of which reached steady-state level after less than 100 ms. The electrical coupling coefficient for the LP to PY synapses tested ($\Delta V_{PY}/\Delta V_{LP}$ in PTX) was $0.0469 \pm 0.0065$ (mean $\pm$ SEM, N=18).

The chemical component of the synapse approximated by subtraction (Ctrl-PTX) consisted of a 3 mV hyperpolarization in response to the first pulse, followed by smaller (< 0.5 mV) hyperpolarizations in response to subsequent pulses. The amplitude difference between the first and subsequent responses indicated that the chemical component showed strong depression. Note that the subtraction of the PTX trace from the control trace produced small transients at the beginning and end of each pulse. These transients were due to the fact that the PY response was faster in PTX than in control, possibly because of a reduction in the membrane time constant.

To examine the dynamics of the LP to PY synapse, we measured the dependence of the PY neuron PSPs on the durations of the interpulse intervals. In general, the responses to the fourth and fifth pulses were identical, indicating that the PSP had reached a stationary state. We thus defined the response to the fifth pulse as the stationary PSP. Figure 2B shows the stationary PSP in response to activation of the LP to PY synapse with a train of voltage pulses, for five different interpulse intervals. As we increased the interpulse interval and allowed more time for recovery from depression, the stationary PSP became less depolarizing. In Fig. 2B, the PSP was purely depolarizing when the interpulse interval was 800 ms or shorter. However, with longer interpulse intervals, the PSP had a hyperpolarizing component. As a result, with longer interpulse intervals, the depolarizing PSP at the end of the pulse was also smaller.

Figure 2B shows that the negative peak of the PY neuron PSP disappeared as the interpulse interval was decreased, thus indicating that the synapse could effectively change sign from negative to positive when the frequency of the presynaptic signal was increased. The negative component of the PSP typically peaked at around 50 to 70 ms after the beginning of the pulse. We thus measured the amplitude of the PSP at 60 ms as a function of the interpulse duration (Fig. 2C, open circles). This amplitude showed a significant change with interpulse duration (one-way ANOVA, N=18, $p<0.0001$) and

changed from positive to negative at an interpulse duration of approximately 4 s. In several cases, the PSP at 60 ms was positive (5 out of 18 cases) or negative (2 out of 18 cases) in sign, at all measured interpulse intervals (data not shown).

The amplitude of the PSP at 60 ms gave us a measure of the strength of the PSP at the beginning of the pulse only. As a more general measure of the strength of the PSP, we calculated the average amplitude of the stationary PSP by integrating the PSP waveform during the presynaptic pulse and dividing by the pulse duration. Figure 2C (filled squares) shows these data for a pulse duration of 400 ms. This plot indicated that the average PSP also decreased with interpulse duration (one-way ANOVA, N=18, $p<0.0001$), but remained positive at all durations measured.

Figure 2 showed that the LP to PY synapse changed sign as a function of interpulse interval. These dynamics arose from an interaction between an electrical and a chemical component. Using the pulse train paradigm described above, we found that the amplitude of the PY responses in PTX did not change even at the shortest interpulse interval (one-way ANOVA, N=18, $p>0.15$, see for example, 2$^{nd}$ trace Fig. 2A). This suggested that the electrical component does not show synaptic depression or facilitation at the interpulse intervals we tested. Hence, we focused on characterizing the frequency dependence of the chemical component.

Activating the synapse with same voltage step injected at different interpulse intervals allowed us to quantify the dynamics of the chemical IPSP (control minus PTX) using paired-pulse paradigm. Figure 3A shows the ratio of the 2$^{nd}$ peak ($A_2$) to the 1$^{st}$ peak ($A_1$) of the IPSP (see inset) as a function of the interpulse interval (IPI) for pulse durations of 200 and 400 ms (mean $\pm$ SEM; N=18). At any IPI, the extent of recovery from depression was larger for the shorter (200 ms) pulses (2-way ANOVA, $p<0.0001$), indicating that there was more recovery when the IPSP had less time to decay.

The relationship between recovery and the IPI is a measure of the time constant of recovery from depression. To quantify this time constant, in each experiment we computed the relationship of recovery and the IPI and fit it with an exponential curve with time constant $\tau_{rec}$. In the example shown in Fig. 3B (mean $\pm$ $\sigma$ across 5 trials) $\tau_{rec}$ = 3.96 s. The y-intercept of the exponential fit ($R_0$ as indicated by the arrow) shows the extent of recovery as IPI tends to 0. Thus, $D_{max} = 1 - R_0$ is a measure of the maximum level of depression for trains of pulses of given duration and amplitude (400 ms and 40 mV, respectively, in Fig. 3B). The exponential fit is given by the equation $1 - D_{\max} e^{-IPI/\tau_{rec}}$. Note that $D_{max} = 0$ corresponds to a non-depressing synapse. Figure 3C is a scatter plot of $\tau_{rec}$ versus $D_{max}$ for 18 PY neurons. As seen in this figure, both parameters were highly variable for different PY neurons. There was a weak negative correlation between the two parameters ($y = -4.7 x + 8.5$; $r = -0.469$; $p < 0.05$, N=18) indicating that the synapses that depressed more recovered faster. Surprisingly,

there was no correlation between the peak amplitude of the initial IPSP ($A_1$ in Fig. 3A inset) and $\tau_{rec}$, indicating that stronger synapses did not recover faster or more slowly (Fig. 3D). Nor was there any correlation between $A_1$ and $D_{max}$ (data not shown).

Although it has been shown that PY neurons can be divided into two groups according to their oscillation phase (Eisen and Marder, 1984), we did not observe any clear division of the time constant and maximum depression of the measured PSPs into two groups. Rather, these parameters were continuously distributed.

*Correlations between the characteristics of the LP to PY PSP and the PY burst phase*

In order to investigate the effect of the LP to PY synapse on the activity of the PY neuron in realistic situations, we measured the correlation of the PY burst phase during the ongoing pyloric rhythm (see Fig. 1C) to several characteristics of the PY neuron PSP (measured after the rhythm was abolished with TTX). We measured the PY burst phase in each preparation during the ongoing pyloric rhythm, before the application of TTX.

Figure 4A and 4B are scatter plots of the PY burst phase ($\Delta T / P_{natural}$) versus peak chemical IPSP and maximum electrical EPSP, respectively (see arrows in inset). The PY burst phase did not show any significant correlation with either parameter. Nor was there any correlation between the peak time of the chemical IPSP and the PY phase (data not shown). In contrast, Fig. 4C shows that the ratio of the peak chemical IPSP to the maximum electrical EPSP was negatively correlated with the PY burst phase ($y = -0.15 x - 0.04$; $r = -0.72$, $p < 0.01$).

The ratio of the peak chemical IPSP to the maximum electrical EPSP is a measure of the relative strengths of the chemical and electrical components of the PSP. This measure, however, does not take into consideration the relative time courses of these two components. To account for the kinetics of the two components, we measured the time at which the first PSP reversed from hyperpolarizing to depolarizing, since all PY synapses tested changed sign during the first pulse. We refer to this time as the zero-cross time (see inset). Figure 4D shows that the PY neuron phase is strongly correlated with the zero-cross time of the PSP ($y = -0.0009 x + 0.02$; $r = 0.854$, $p < 0.001$).

The correlations between the PY phase and both the zero-cross time and the ratio of the peak chemical IPSP to the maximum electrical EPSP indicated that the relative strength and kinetics of the two PSP components could reliably predict the contribution of LP to the bursting phase of PY. Thus, those PY neurons whose PSP switched sign at a later time, or had a strong chemical versus electrical component, tended to burst at a later phase.

Traditionally, the firing phase of individual pyloric neurons is computed with respect to the burst onset of the pacemaker neurons AB and PD. However, in our study there was no significant correlation between the parameters of the LP to PY PSP and the PY burst phase in an ongoing rhythm, when measured with respect to the PD neuron (data not shown). This is not surprising since the timing between the burst of the PD neuron and the PY neuron can be influenced by many factors other than the LP to PY synapse, such as the synapse from the AB neuron and the PD neuron to the PY neuron (Eisen and Marder, 1984).

*Synaptic dynamics in response to the realistic waveforms*

Up till now we have investigated the properties of the LP to PY synapse by activating the synapse with square voltage pulses. However, graded synapses are known to show different responses depending on the shape of the membrane potential waveform of the presynaptic cell (Olsen and Calabrese, 1996; Manor et al., 1997; Simmons, 2002). Hence, to examine the role of the LP to PY synapse in realistic conditions, we studied the dynamics of the synapse by activating it with realistic LP waveforms. Two sets of realistic waveforms were constructed (see Methods) by recording LP voltage traces during slow and fast pyloric rhythms and low-pass filtering the waveform at 10 Hz (Fig. 5; top two traces). Only these two waveforms (with the cycle period indicated) were used in the current study.

After the ongoing rhythm was abolished with bath application of TTX, 10 repetitions of the resulting waveforms were played back into the LP neuron in voltage clamp (from a holding potential of –60 mV) and the PSPs were recorded from the PY neuron. Figure 5 (bottom traces) shows an example of the PSPs recorded from the PY neuron when the LP to PY synapse was activated with repetitive applications of realistic LP waveforms. The initial small peak in the PSPs in response to the short-period waveform was seen in a few cases and was due to the slight delay of the activation of the chemical synapse with respect to the electrical synapse.

Note that, after several cycles of the waveform, the individual PSPs in response to each cycle of the realistic waveform were identical in shape and size and always depolarizing. This was true even when the PSP in response to the first one or two cycles of the waveform was hyperpolarizing. In our analysis we use the PY PSPs measured after the $5^{th}$ cycle of the realistic waveform.

We examined the role of chemical inhibition by comparing the PSP recorded in the absence of chemical synapse (marked PTX) with those recorded in control conditions. Figure 6A shows an example of such a comparison for the short-period LP waveform. Although in both control and PTX the PSPs were depolarizing, their peak times (measured from the peak of the LP waveform to the peak of the PSP) and peak amplitudes were different. In PTX, the peak PSP occurred earlier and was larger, suggesting that the chemical component of the synapse acted to delay and decrease the amplitude of the PSP ($p < 0.005$, *t*-test,

N=9 for both the delay of the peak and the reduction of the amplitude; Fig 6Bi). Similar results were obtained with the long-period LP waveform ($p < 0.005$, *t*-test, N=9 for both the delay of the peak and the reduction of the amplitude; Fig. 6Bii).

One of our main hypotheses is that the PY PSP in response to the realistic LP waveform is important in determining the activity of PY neurons during an ongoing rhythm. A direct examination of this contribution was not possible since we record the PSP in PY neurons after blocking rhythmic pyloric activity and playing back the LP waveform in the voltage-clamped LP neuron. Thus, we decided to look for correlations between the PSP in PY neurons, recorded in the absence of activity, and the activity of the same PY neurons in relationship to the LP neuron *before* the rhythmic activity was blocked. Moreover, the results described in Fig. 6 indicated that one contribution of the chemical component was to delay the peak of the PSP. We thus investigated correlations between the peak phase of the PSP and the activity of the PY neuron in an ongoing pyloric rhythm. The peak phase of the PY PSP was measured as the time difference (dt) between the peak of the injected realistic LP waveform and the peak of the PSP, divided by the waveform period $P_{applied}$ (Fig. 7A). For each PY neuron, the peak phase of the PY was calculated for both the PSP in response to the short-period LP waveform and that in response to the long-period waveform. As a measure of the activity of the PY neuron in the ongoing pyloric rhythm, we used the phase $\Delta T / P_{natural}$ of the PY burst onset with respect to the LP burst onset (as in Fig. 4; also see Fig. 1C).

The PY phase ($\Delta T / P_{natural}$) was significantly correlated to both the peak phase of the PSP in response to the short-period waveform (Fig. 7B; $y = 0.6 x + 0.01$; $r = 0.667$, $p < 0.05$, $N = 12$) and the peak phase of the PSP in response to the long-period waveform (Fig. 7C; $y = 0.41 x + 0.07$; $r = 0.644$, $p < 0.05$, $N = 12$). These correlations indicate that a later peak in the LP to PY PSP corresponded to a later burst phase (with respect to LP) of the PY neuron in the ongoing rhythm, and that such a relationship holds for both the PSP in response to short-period and long-period waveforms.

## Discussion

Coordination between the firing times of different motoneurons participating in a rhythmic motor behavior is vital for producing meaningful behavior. When cycle period changes, the intervals between firing times of motoneurons must be adjusted to maintain the basic structure of the pattern. The pyloric circuit in *Panulirus interruptus* is an example where cycle period can change several fold, yet the tri-phasic structure of the rhythm is relatively well conserved. In this work we described the temporal dynamics of a mixed synapse between two members of this network, the LP and PY neurons, and showed how these complex dynamics could affect the phasing between the two neurons, in response to changes in cycle period.

The synapse from the LP to the PY neuron consists of an inhibitory chemical component that shows depression, and an electrical component that is frequency-independent. We show that when the LP neuron is activated with low frequencies, the LP to PY synapse has an initial inhibitory (hyperpolarizing) and a later excitatory (depolarizing) component. At higher frequencies, the effect of the LP to PY synapse is always excitatory since the chemical component of the synapse is mostly depressed. Previous studies have shown that differential neuromodulation of the chemical and electrical components could lead to sign reversal at a mixed synapse (Graubard and Hartline, 1987; Johnson et al., 1993). To our knowledge, our study is the first example to show that such a synapse can reverse its sign as an automatic response to a change in frequency of the presynaptic neuron.

*The activity phase of PY neurons in an ongoing rhythm is correlated with the balance of electrical and chemical components of the LP to PY synapse.*
In the pyloric circuit of *Panulirus interruptus,* there are 6-8 PY neurons, identified by their projections to the pyloric muscles and their connectivity to other pyloric neurons. Nevertheless, within the same preparation, the firing times of PY neurons show some variability. Previous studies have categorized PY neurons into two groups, those that fire early or late in the pyloric (Hartline and Gassie, 1979; Eisen and Marder, 1984). However, when we computed the firing phase of different PY neurons with reference to the LP neuron firing time, we did not see two well-defined groups of PY neurons but a continuum of phases.

Interestingly, however, we found a correlation between the characteristics of the isolated LP to PY synapse and the phase of the PY neuron in an ongoing rhythm. When a single voltage pulse was injected into the LP neuron, the PSP in the PY neuron switched from hyperpolarizing (chemical IPSP) to depolarizing (electrical EPSP) during the pulse. Two characteristics of this mixed PSP, the zero-cross time and the ratio of the peak of the chemical IPSP and the maximum electrical EPSP, correlated well with the bursting phase of the PY neuron. Both characteristics are determined by the interactions among many factors, including

the relative strengths of the chemical and electrical synapses and the rates and extent of depression and recovery of the chemical synapse. However, each of these components alone did not show any significant correlation with the bursting phase of the PY neuron.

These correlations showed that those PY neurons whose PSP switched sign at a later time, or had a stronger chemical versus electrical component, tended to burst at a later phase. Hence, the variability in PY phases, which we observed in ongoing pyloric rhythms, could be due to differences in the relative strength of chemical inhibition and electrical excitation. It is not known what mechanism could be responsible for such differences, but several possibilities can be raised. For instance, it is possible that the chemical and electrical components affect the PY neurons at different morphological sites, or that the electrical coupling conductance or the dynamics of the chemical component varies for different PY neurons.

*Contribution of the LP to PY synapse to the activity phase of the PY neurons in an ongoing pyloric rhythm*

The ideal way to quantify the synaptic influence of the LP neuron on the PY neurons is to measure the strength (amplitude) and dynamics (time-to-peak) of the LP to PY PSP in an ongoing rhythm. However, since PY neurons receive synaptic inputs from other neurons and have voltage-gated ionic conductances, it is difficult to isolate the effect of the LP to PY synapse in an ongoing rhythm. As a close approximation, we played back pre-recorded realistic LP waveforms into the voltage-clamped LP neuron and measured the postsynaptic potential in the PY neuron.

When the LP neuron was periodically stimulated with a realistic waveform, the total effect of the LP to PY synapse was a repetitive depolarization in the PY neuron. Thus, it appears that in an ongoing rhythm the LP to PY synapse acts to *advance* the PY burst of activity by depolarizing the PY neuron. Yet, the chemical component of the synapse is not totally depressed but has some contribution. This component acts to *delay* the burst of the PY neuron, and possibly decrease its amplitude. It is thus reasonable to conclude that, in an ongoing rhythm, these two opposing effects fine-tune the burst phase of PY neurons in a manner that strongly depends of the cycle period. Indeed, when the LP neuron was injected with realistic waveforms of different frequencies, the PY neuron PSP followed with some delay that was larger with the larger cycle period. This effect is due to the frequency-dependent dynamics of the chemical component of the LP to PY synapse. In an ongoing rhythm, it is expected that both effects combine to increasingly delay the burst of the PY neurons if cycle period increases. What are the functional implications of such an effect to the phasing of PY neurons?

Previous studies have computed the activity phase of different neurons in the pyloric cycle (Hooper, 1997a; 1997b). In these studies, it was found that across different cycle frequencies the LP (as well as PY) neuron burst onsets did

not occur at a fixed phase with respect to the pacemaker neurons. As cycle frequency was increased from 0.5 to 2.5 Hz, both the LP and the PY neuron bursts occurred at later phases. Interestingly, however, in this frequency range the phase difference between the LP and PY neuron bursts was nearly constant (Hooper, 1997b). The present work shows that the peak time of the LP to PY PSP is delayed if the period of the LP waveform is increased. This is consistent with the hypothesis that the dynamics of the LP to PY synapse work to maintain an approximately fixed phase between the LP and PY neurons, across different cycle periods.

*The Interaction of rectifying electrical and depressing chemical components of the LP to PY synapse facilitates, and then delays, the onset of a PY burst.*
At first sight, having the same presynaptic neuron exert two opposing effects on the postsynaptic cell seems puzzling. But do these two effects occur at the same time? In our experiments, we measured the dynamics of the LP to PY synapse in TTX when the neurons were quiescent. In these conditions, realistic waveforms injected into the LP neuron produced a total depolarizing effect on the PY neuron. However, when considering an ongoing rhythm, this simplified effect must be revised. In an ongoing rhythm, both LP and PY neuron membrane potentials are oscillating. Since the electrical synapse between the LP and PY neurons is rectifying (Graubard and Hartline, 1987), the LP neuron can pass a depolarizing coupling current to the PY neuron only during a limited part of the cycle –when it is at more positive membrane potential than the PY neuron. During other parts of the cycle, no current passes from the LP neuron to the PY neuron through the electrical synapse. Moreover, two other factors may affect the electrical/chemical ratio of the mixed synapse. First, PY neurons that fire at an earlier phase tend to have higher electrical/chemical ratio and faster depressing chemical synapse, but since they burst early during ongoing rhythm, the electrical coupling effect is shut off early (due to rectification) as well. Second, at the onset of a PY neuron burst, as its membrane potential depolarizes, the driving force of the inhibition increases thus making the chemical component stronger. We propose that, in an ongoing rhythm, the depolarizing effect of the electrical component is prominent only during the initial stages of the LP burst and is important to induce the PY burst. In the latter part of the LP burst, the chemical component of the LP to PY synapse becomes more significant, and acts to fine-tune the burst time of the PY neuron according to cycle frequency. These effects can be shown in a computational model of the mixed synapse (Nadim, Mamiya and Manor, *In preparation*).

Ideally, one could unmask the contribution of the electrical component of the LP to PY synapse by blocking the chemical component during ongoing pyloric activity. However, many chemical synapses within the pyloric network (including the AB to LP synapse) and many descending inputs to the stomatogastric ganglion are blocked by picrotoxin. Thus, bath application of picrotoxin in an ongoing rhythm has many confounding effects and the results are not easily interpreted.

*Conclusions*

We have shown that in an oscillatory network a mixed synapse could have significant influences on the activity of the postsynaptic neuron. First, because the chemical component is frequency dependent and the electrical component is relatively constant, the total effect depends on the frequency and in some cases it can reverse its sign. Second, when the electrical synapse is rectifying, the effect of the electrical component is restricted to a brief window in the cycle. Hence, the effect of electrical excitation and chemical inhibition may be temporally separate. We propose that, at this synapse, both excitation and inhibition are required for the normal phasing of PY neurons, but at different times. The combination of depressing chemical inhibition and rectifying electrical excitation satisfies this requirement.

**Figure Legends**

**Figure 1.** *The pyloric network generates a triphasic rhythm*. **A.** Intracellular voltage traces from the pyloric network pacemaker neuron AB, the LP and two PY neurons. Bursting activity in the AB neuron is followed, with a delay, by a burst of action potentials in the LP neuron and, with some overlap, by bursts of action potentials in the PY neurons. **B**. Circuit diagram shows the connectivity among the AB, PD, LP and PY neurons. Stimulating and recording electrodes were used in the LP neuron. Recording electrodes were used to monitor the PY responses. **C.** Diagram indicating how phase of the PY neuron burst onset was calculated with respect to the LP neuron burst onset during an ongoing pyloric activity. The phase is equal to the time difference ($\Delta T$) between the two burst onsets divided by the pyloric cycle period ($P_{natural}$).

**Figure 2.** *Postsynaptic potential of PY in response to stimulation of the LP neuron with trains of voltage pulses*. **A.** A train of five 40 mV voltage pulses were injected in the LP neuron. Ctl and PTX traces show the voltage response of a PY neuron in control and in 10 $\mu$M picrotoxin that blocked the LP to PY chemical component. Ctl-PTX trace shows the chemical component of the LP to PY synapse, obtained by subtracting the Ctl and PTX traces. **B.** The voltage response of the PY neuron at the fifth pulse was defined as the stationary PSP. Shown are stationary PSPs for different interpulse durations (400 ms, 800 ms, 2 s, 4 s, and 8 s). **C.** Amplitude of the stationary PSP (mean $\pm$ SEM; N=18) as a function of the interpulse interval, measured at 60 ms from the pulse onset (open circles) and as average (integral/pulse duration, filled squares).

**Figure 3.** *Recovery and depression of the chemical component of the LP to PY synapse*. **A.** A paired-pulse paradigm was used to measure the extent of synaptic recovery as function of interpulse interval (inset). All presynaptic pulses were 40 mV in amplitude. The peak ratio of second chemical IPSP ($A_2$) to first chemical IPSP ($A_1$) was plotted as function of interpulse interval (IPI), for two different pulse durations (mean $\pm$ SEM; N=18; open squares, 200 ms; filled circles, 400 ms). **B.** In each experiment, the ratio $A_2/A_1$ versus ISI was fit with a single

exponential fit. In this example with pulse durations of 400 ms, the exponential fit of the recovery plot (mean±σ; n=5 trials) gave an estimation of 3.96 for the time constant of recovery. The y-intercept of this exponential curve (R0) shows the extent of recovery as IPI tends to 0, and $D_{max}$=1 - R0 represents the maximum level of depression for this case. **C.** Time constant of recovery as function of maximum level of depression (mean ± SEM; N=18). Solid line represents a linear correlation (r=0.469, p<0.05). **D.** The time constant of recovery did not show any correlation with the peak chemical IPSP.

**Figure 4.** *PY burst phase correlates with some dynamic parameters of the LP to PY synapse*. PY burst phase was measured in the on-going pyloric rhythm, as the ratio of Δt (time interval between bursts onsets of LP and PY neurons) and P (the pyloric period). Dynamical parameters of the LP to PY synapse were measured after blocking pyloric activity, where the LP neuron was stimulated with a train of voltage pulses. Schematic insets show how these parameters were obtained from PY PSP responses. The PY burst phase was not correlated with the peak chemical IPSP (A) or the maximal electrical EPSP (B), but was strongly correlated with the ratio of the peak chemical IPSP to the maximal electrical EPSP (C; r=-0.72, p<0.01) and the zero cross time (D; r=0.854, p<0.001).

**Figure 5.** *Construction of realistic waveforms*. The pyloric frequency was modified by injecting current into the pacemaker neurons (AB/PD). Typical short-period (625 ms, top left trace) and long-period (1600 ms, top right trace) waveforms were recorded in the LP neuron and low-pass filtered at 10 Hz to produce smooth unitary waveforms (middle traces). The resulting waveforms were played back into the voltage-clamped LP neuron (see text) and the post-synaptic potentials were measured in the PY neuron (bottom traces).

**Figure 6.** *The LP to PY chemical inhibition decreases the amplitude and delays the peak of the PSP in PY*. **A.** A pre-recorded realistic LP waveform was played back in the voltage-clamped LP neuron and the PY PSP was recorded in control conditions (solid line) and in the presence of 10 μM picrotoxin (dashed line). The example shown is the response to a short period waveform. Circles and arrows label the PSP peak amplitudes and peak times (from the peak of the presynaptic LP waveform). The peak amplitude and peak time were significantly different in control and in PTX (p<0.005, t-test, N=9), both for the short period (**Bi**) and for the long period (**Bii**) LP waveform.

**Figure 7.** *Correlation between phase of PY PSP to phase of PY burst in an on-going rhythm*. A. The phase of the PY PSP was measured as the ratio of the interval between the peak times of the LP waveform and the PY PSP (dt) and the cycle period (P). **Bi.** The PY burst phase in the ongoing rhythm (see text and legend of Fig. 4) was plotted against the PY PSP phase, when LP was injected with a short-period waveform (P=625 ms). Linear regression fit: p<0.05, n=12, r=0.667. **Bii.** Same as Bi, when LP was injected with a long-period waveform (P=1600 ms). Linear regression fit: p<0.05, n=12, r=0.644.

## References


Benardo LS (1997) Recruitment of GABAergic inhibition and synchronization of inhibitory interneurons in rat neocortex. J Neurophysiol 77:3134-3144.

Eisen JS, Marder E (1984) A mechanism for production of phase shifts in a pattern generator. J Neurophysiol 51:1375-1393.

Fukuda T, Kosaka T (2000) Gap junctions linking the dendritic network of GABAergic interneurons in the hippocampus. J Neurosci 20:1519-1528.

Galarreta M, Hestrin S (1999) A network of fast-spiking cells in the neocortex connected by electrical synapses. Nature 402:72-75.

Galarreta M, Hestrin S (2001a) Spike transmission and synchrony detection in networks of GABAergic interneurons. Science 292:2295-2299.

Galarreta M, Hestrin S (2001b) Electrical synapses between GABA-releasing interneurons. Nat Rev Neurosci 2:425-433.

Gibson JR, Beierlein M, Connors BW (1999) Two networks of electrically coupled inhibitory neurons in neocortex. Nature 402:75-79.

Graubard K, Hartline DK (1987) Full-wave rectification from a mixed electrical-chemical synapse. Science 237:535-537.

Harris-Warrick RM, Marder E, Selverston AI, Moulins M (1992) Dynamic Biological Networks. The Stomatogastric Nervous System. Cambridge: MIT Press.

Hartline DK, Gassie DV, Jr. (1979) Pattern generation in the lobster (Panulirus) stomatogastric ganglion. I. Pyloric neuron kinetics and synaptic interactions. Biol Cybern 33:209-222.

Hooper SL (1997a) Phase maintenance in the pyloric pattern of the lobster (*Panulirus interruptus*) stomatogastric ganglion. J Comput Neurosci 4:191-205.

Hooper SL (1997b) The pyloric pattern of the lobster (*Panulirus interruptus*) stomatogastric ganglion comprises two phase maintaining subsets. J Comput Neurosci 4:207-219.

Johnson BR, Peck JH, Harris-Warrick RM (1993) Dopamine induces sign reversal at mixed chemical-electrical synapses. Brain Res 625:159-164.

Mann-Metzer P, Yarom Y (1999) Electrotonic coupling interacts with intrinsic properties to generate synchronized activity in cerebellar networks of inhibitory interneurons. J Neurosci 19:3298-3306.

Manor Y, Nadim F, Abbott LF, Marder E (1997) Temporal dynamics of graded synaptic transmission in the lobster stomatogastric ganglion. J Neurosci 17:5610-5621.

Marder E, Paupardin-Tritsch D (1978) The pharmacological properties of some crustacean neuronal acetylcholine, gamma-aminobutyric acid and l-glutamate responses. J Physiol 280:213-236.

Michelson HB, Wong RK (1994) Synchronization of inhibitory neurones in the guinea-pic hippocampus in vitro. J Physiol (Lond) 477:35-45.

Miller JP, Selverston AI (1982) Mechanisms underlying pattern generation in lobster stomatogastric ganglion as determined by selective inactivation of

identified neurons. IV. Network properties of pyloric system. J Neurophysiol 48:1416-1432.
Nusbaum MP, Beenhakker MP (2002) A small-systems approach to motor pattern generation. Nature 417:343-350.
Olsen OH, Calabrese RL (1996) Activation of intrinsic and synaptic currents in leech heart interneurons by realistic waveforms. J Neurosci 16:4958-4970.
Selverston AI, Russell DF, Miller JP (1976) The stomatogastric nervous system: structure and function of a small neural network. Prog Neurobiol 7:215-290.
Simmons P (2002) Presynaptic depolarization rate controls transmission at an invertebrate synapse. Neuron 35:749.
Tamas G, Buhl EH, Lorincz A, Somogyi P (2000) Proximally targeted GABAergic synapses and gap junctions synchronize cortical interneurons. Nat Neurosci 3:366-371.

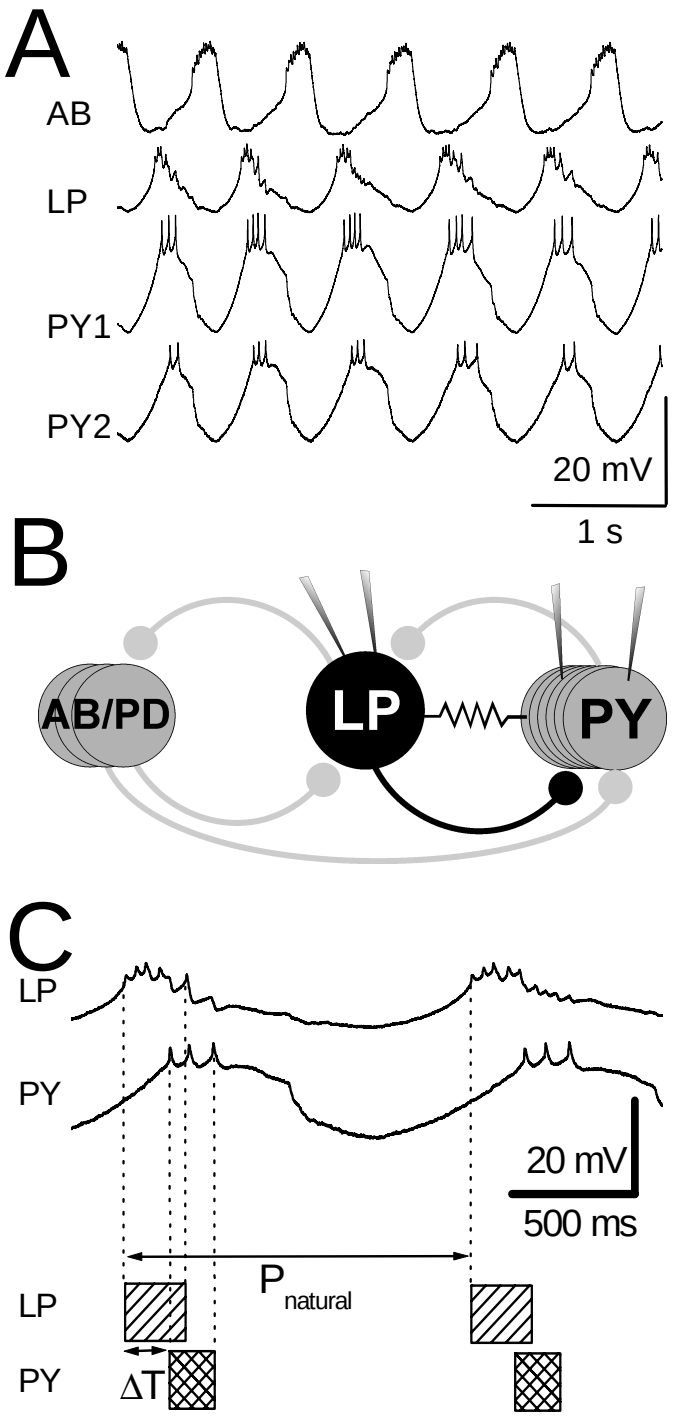
A
AB
LP
PY1
PY2
20 mV
1 s
B
AB/PD
LP
PY
C
LP
PY
20 mV
500 ms
P natural
LP
PY
ΔT

Figure 1

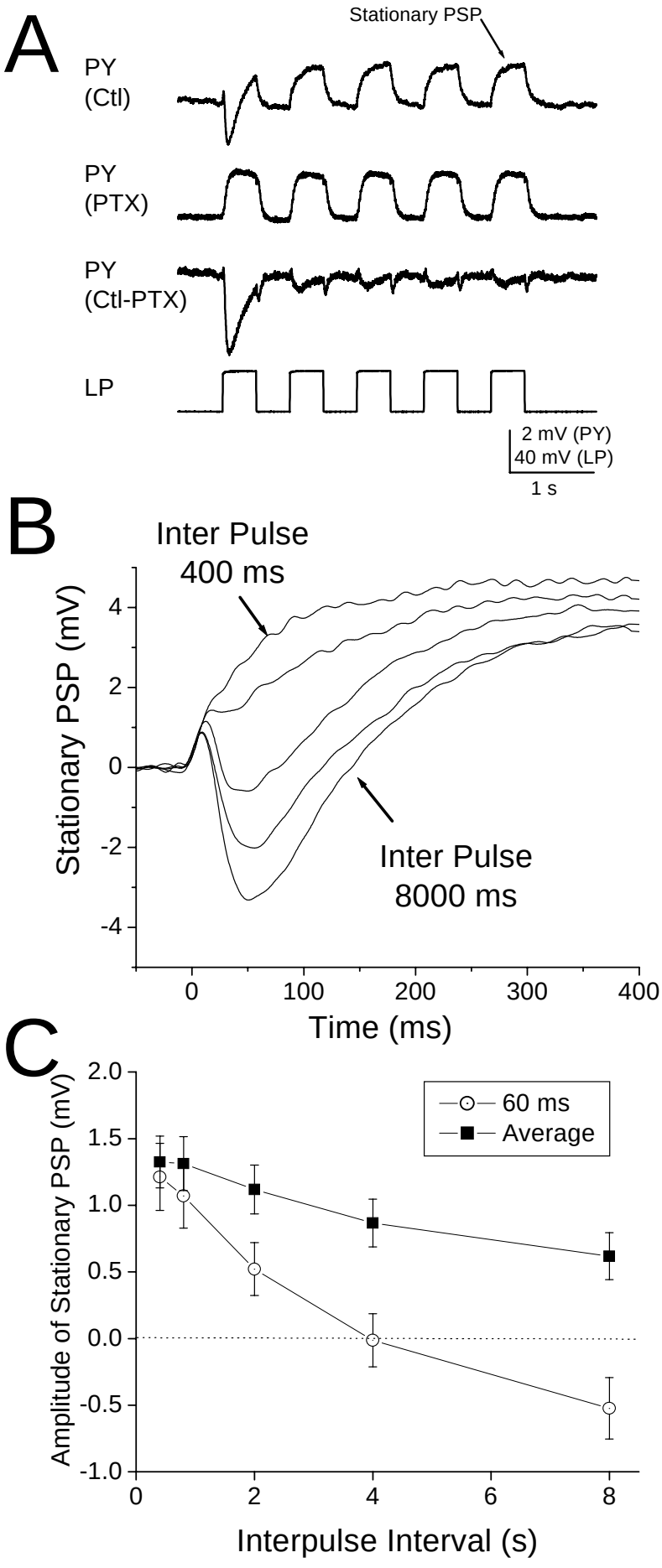
A
Stationary PSP
PY
(Ctl)
PY
(PTX)
PY
(Ctl-PTX)
LP
2 mV (PY)
40 mV (LP)
1 s
B
Inter Pulse
400 ms
Inter Pulse
8000 ms
Stationary PSP (mV)
Time (ms)
C
60 ms
Average
Amplitude of Stationary PSP (mV)
Interpulse Interval (s)

Figure 2

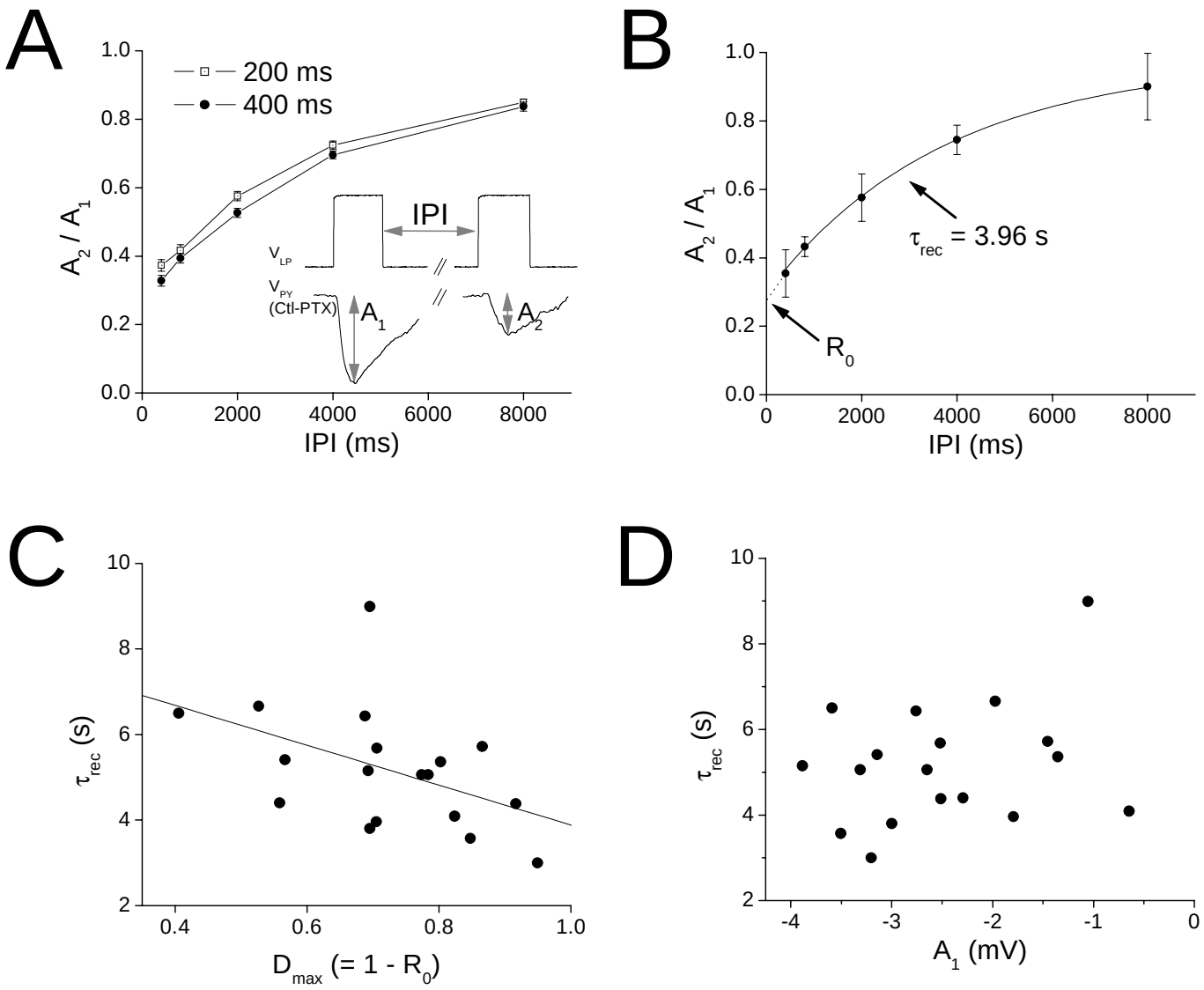
A
200 ms
400 ms
A2 / A1
IPI
VLP
VPY
(Ctl-PTX)
A1
A2
IPI (ms)
B
τrec = 3.96 s
R0
C
τrec (s)
Dmax (= 1 - R0)
D
A1 (mV)

Figure 3

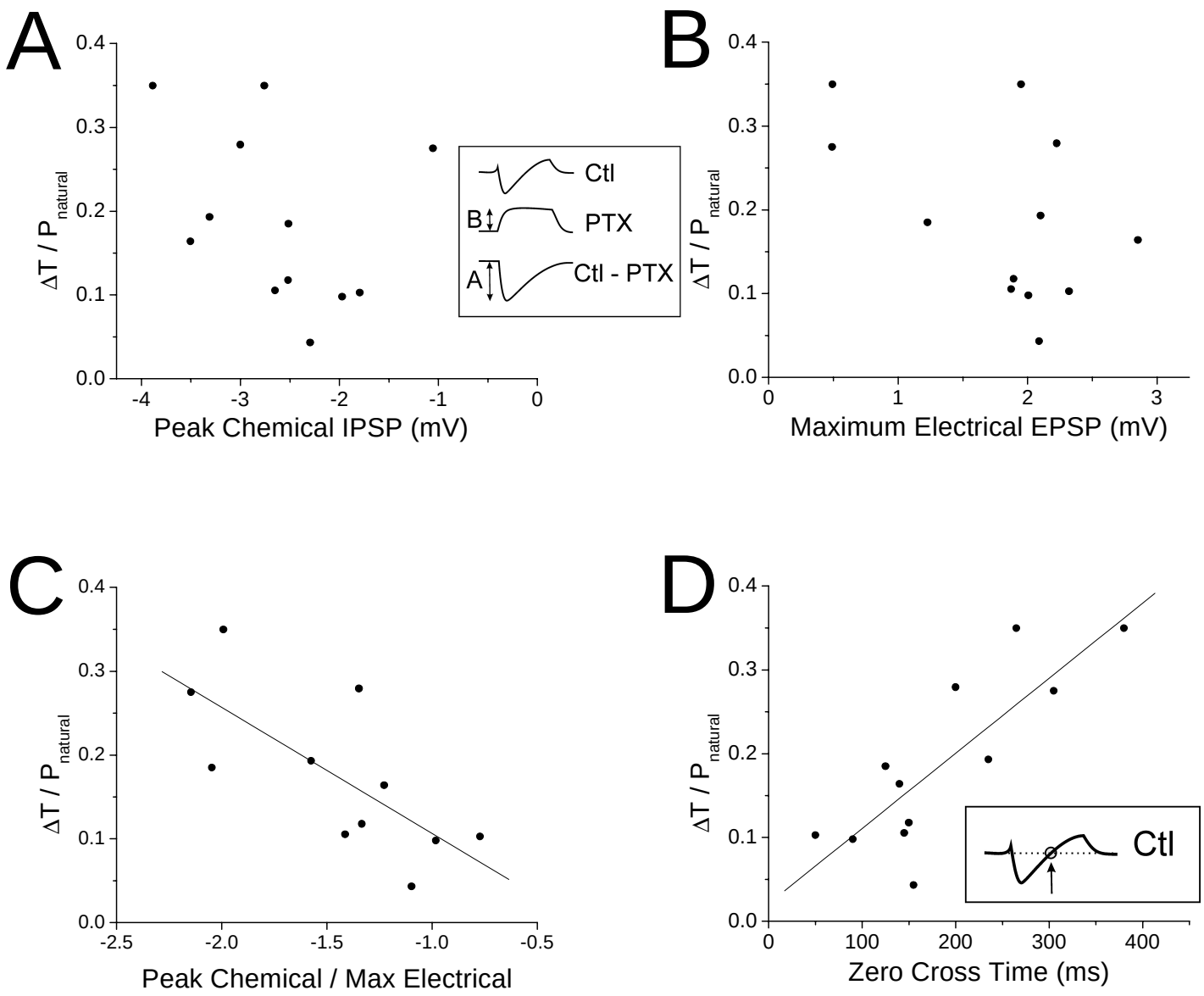
A
B
C
D
ΔT / P natural
Peak Chemical IPSP (mV)
Maximum Electrical EPSP (mV)
Peak Chemical / Max Electrical
Zero Cross Time (ms)
Ctl
PTX
Ctl - PTX
B
A

Figure 4

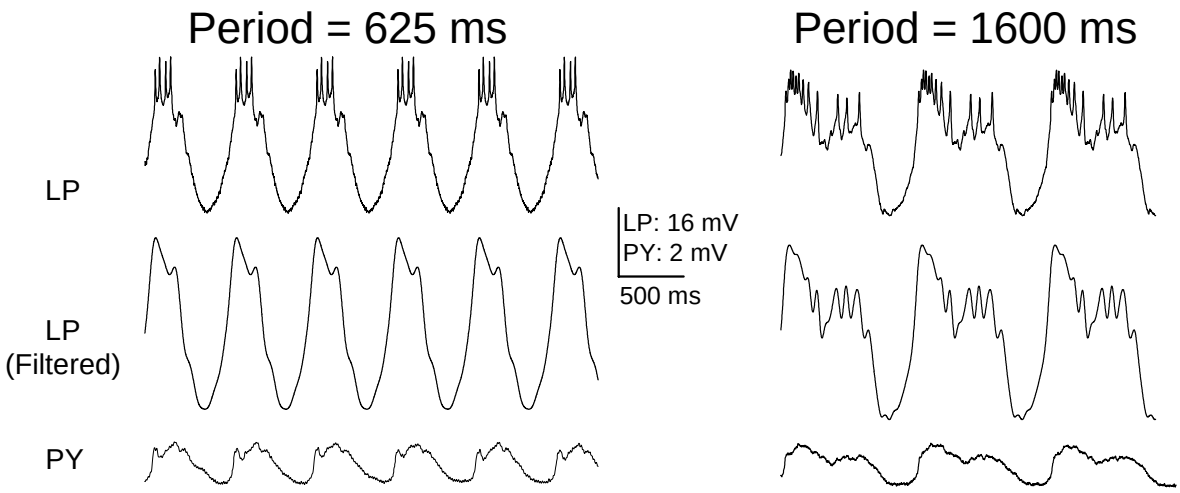
Period = 625 ms
Period = 1600 ms
LP
LP
(Filtered)
PY
LP: 16 mV
PY: 2 mV
500 ms

Figure 5

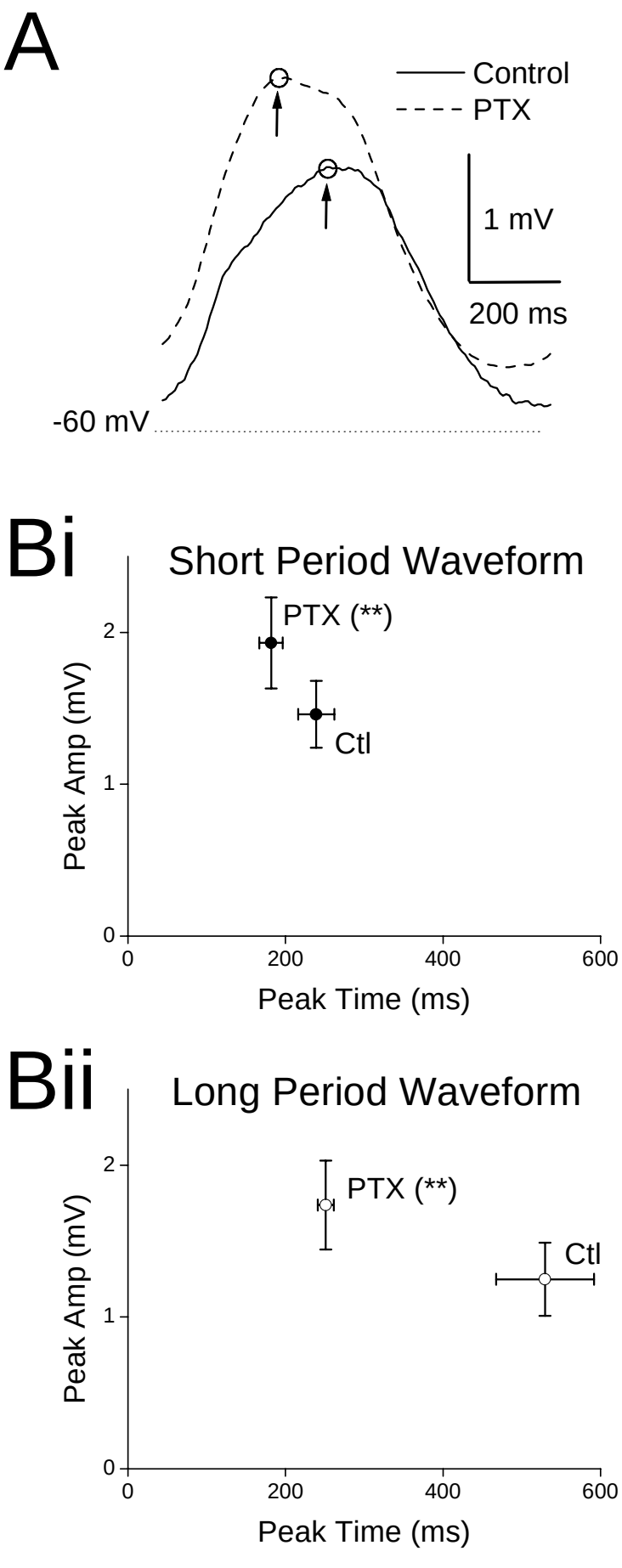
A
Control
PTX
1 mV
200 ms
-60 mV
Bi
Short Period Waveform
PTX (**)
Ctl
Peak Amp (mV)
Peak Time (ms)
Bii
Long Period Waveform
PTX (**)
Ctl
Peak Amp (mV)
Peak Time (ms)

Figure 6

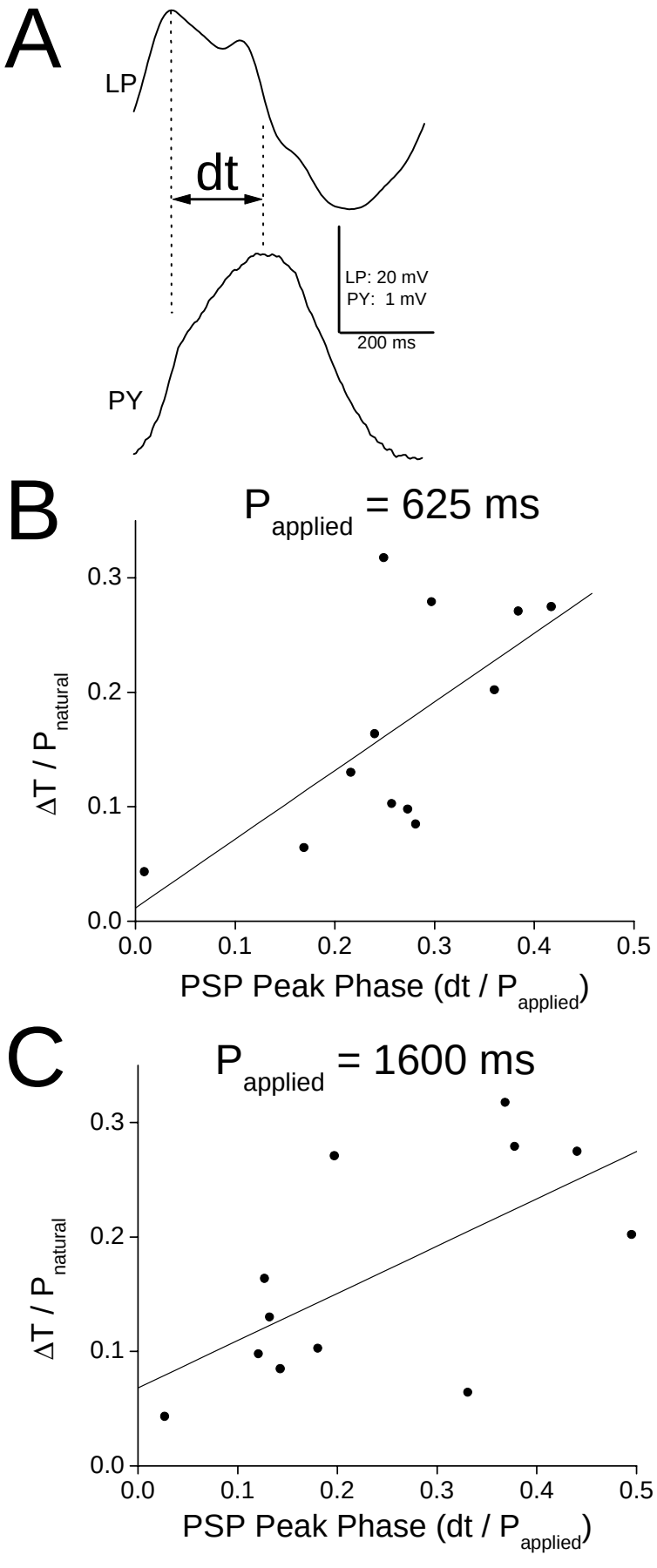
A
LP
dt
LP: 20 mV
PY: 1 mV
200 ms
PY
B
P applied = 625 ms
ΔT / P natural
PSP Peak Phase (dt / P applied)
C
P applied = 1600 ms
ΔT / P natural
PSP Peak Phase (dt / P applied)

Figure 7